Human Molecular Genetics, 2015, Vol. 24, No. 2 **506–515**
doi:10.1093/hmg/ddu470
Advance Access published on November 16, 2014

Convulsive seizures and SUDEP in a mouse model of *SCN8A* epileptic encephalopathy

Jacy L. Wagnon[1], Matthew J. Korn[2], Rachel Parent[3], Taylor A. Tarpey[3], Julie M. Jones[1], Michael F. Hammer[4], Geoffrey G. Murphy[3,5], Jack M. Parent[2,6] and Miriam H. Meisler[1,2,*]

[1]Department of Human Genetics, [2]Department of Neurology, [3]Molecular and Behavioral Neuroscience Institute, University of Michigan, Ann Arbor, MI 48109, USA, [4]Arizona Research Laboratories, Division of Biotechnology, University of Arizona, Tucson, AZ, USA, [5]Molecular and Integrative Physiology, University of Michigan Medical Center, Ann Arbor, MI 48109, USA and [6]VA Ann Arbor Healthcare System, Ann Arbor, MI, USA

Received June 19, 2014; Revised August 14, 2014; Accepted September 9, 2014

***De novo* mutations of the voltage-gated sodium channel gene *SCN8A* have recently been recognized as a cause of epileptic encephalopathy, which is characterized by refractory seizures with developmental delay and cognitive disability. We previously described the heterozygous *SCN8A* missense mutation p.Asn1768Asp in a child with epileptic encephalopathy that included seizures, ataxia, and sudden unexpected death in epilepsy (SUDEP). The mutation results in increased persistent sodium current and hyperactivity of transfected neurons. We have characterized a knock-in mouse model expressing this dominant gain-of-function mutation to investigate the pathology of the altered channel *in vivo*. The mutant channel protein is stable *in vivo*. Heterozygous *Scn8a*$^{N1768D/+}$ mice exhibit seizures and SUDEP, confirming the causality of the *de novo* mutation in the proband. Using video/EEG analysis, we detect ictal discharges that coincide with convulsive seizures and myoclonic jerks. Prior to seizure onset, heterozygous mutants are not defective in motor learning or fear conditioning, but do exhibit mild impairment of motor coordination and social discrimination. Homozygous mutant mice exhibit earlier seizure onset than heterozygotes and more rapid progression to death. Analysis of the intermediate phenotype of functionally hemizygous *Scn8a*$^{N1768D/-}$ mice indicates that severity is increased by a double dose of mutant protein and reduced by the presence of wild-type protein. *Scn8a*^{N1768D} mutant mice provide a model of epileptic encephalopathy that will be valuable for studying the *in vivo* effects of hyperactive $Na_v1.6$ and the response to therapeutic interventions.**

INTRODUCTION

Epileptic encephalopathies are characterized by early onset of refractory seizures and progressive cerebral dysfunction leading to behavioral and cognitive disabilities (1). These heterogeneous disorders are usually diagnosed in infants and children and often result from *de novo* gene mutations (2–5). The mutations affect genes that function in development, synaptic transmission, metabolism, and neuronal signaling, including several voltage-gated sodium channel genes (6,7). More than 80% of individuals with Dravet syndrome carry *de novo* mutations of sodium channel *SCN1A,* and a small number of *SCN2A* mutations have also been described (8). A *de novo* mutation of *SCN8A*, p.Asn1768Asp (N1768D), was identified in 2012 in a child with epileptic encephalopathy (9). The proband exhibited seizure onset at 6 months followed by developmental delay, ataxia and sudden unexpected death in epilepsy (SUDEP) at the age of 15 years. Since the initial report, >18 additional *de novo* mutations of *SCN8A* have been described in this disorder (2,3,10–15), and several others have been identified.

SCN8A encodes the voltage-gated sodium channel $Na_v1.6$, a major neuronal sodium channel in the CNS and PNS that is concentrated at the axon initial segment and at nodes of Ranvier

*To whom correspondence should be addressed at: 4909 Buhl Box 5618, University of Michigan, Ann Arbor, MI 48109-5618, USA. Tel: +1 734763 5546; Fax: +734763 9691; Email: meislerm@umich.edu

(16–19). $Na_v1.6$ is expressed in both excitatory and inhibitory neurons and regulates neuronal signaling by controlling the initiation and propagation of action potentials (20–22). The *SCN8A* mutation N1768D is a gain-of-function mutation that causes a large increase in persistent sodium current leading to neuronal hyperexcitability (9). Previous mouse models of $Na_v1.6$ were limited to loss-of-function mutants that reduce neuronal firing and tend to suppress spontaneous seizures (reviewed in 12). We generated a knock-in mouse carrying the N1768D mutation using TALEN technology in combination with a targeting vector (23), in order to model human epileptic encephalopathy and study the effects of an $Na_v1.6$ gain-of-function mutation *in vivo*.

We now report that the N1768D mutation of *SCN8A* is sufficient to induce seizures and SUDEP in knock-in mice. The mutant mice have convulsive seizures and abnormal EEG patterns that resemble the human condition. Dosage of the mutant *Scn8a* allele is directly correlated with disease severity in the mice, and the presence of the wild-type allele partially attenuates the phenotype. Thus $Scn8a^{N1768D}$ mutant mice provide a robust model of a rare form of severe childhood epileptic encephalopathy.

RESULTS

Reduced lifespan of $Scn8a^{N1768D}$ mutant mice

The p.Asn1768Asp mutation is located in the last transmembrane segment of the $Na_v1.6$ channel (Fig. 1A). The mutated asparagine residue is evolutionarily conserved in vertebrate and invertebrate sodium channels (9). To evaluate the viability of homozygous D/D and heterozygous D/+ mutants, we carried out crosses between D/+ heterozygotes. (We designate the mutant allele 'D' for aspartate). Offspring were genotyped by PCR/RFLP using the *Hinc*II site that was introduced into the mutant allele (23). Digestion with *Hinc*II cleaves the 327 bp mutant PCR product into fragments of 209 and 118 bp (Fig. 1B). The yield of +/+ (6), D/+ (25) and D/D (11) offspring was consistent with the predicted Mendelian ratio of 1:2:1 ($P = 0.25$).

Homozygous D/D mice exhibit a fine motor tremor shortly after birth but are otherwise indistinguishable from wild-type littermates during the first 2 weeks of life. Histological analysis did not detect any gross brain malformation in D/D mice (Fig. 1C). At the age of 18–22 days, there is a precipitous decline of motor function in D/D mice that begins with abnormal gait and progresses to uncoordinated limb movements and loss of righting reflex as shown in the video included in Supplementary Material. Within 24 h, these motor deficits are followed by seizure onset and a single, terminal tonic–clonic seizure. The median age at seizure-induced death is 3 weeks for D/D homozygotes (Fig. 1E).

Heterozygous D/+ mice appear phenotypically normal for the first 2–3 months of age. After seizure onset, D/+ mice experience up to three seizures per day and progress to SUDEP within 1 month (Fig. 1E). The seizure phenotype demonstrates incomplete penetrance, and 50% of D/+ mice show no evidence of seizures within the first 6 months (Fig. 1E). Among the D/+ mice that develop seizures, the median age of death is 4 months. The features of seizure onset and progression in D/D and D/+ mice are summarized in Table 1.

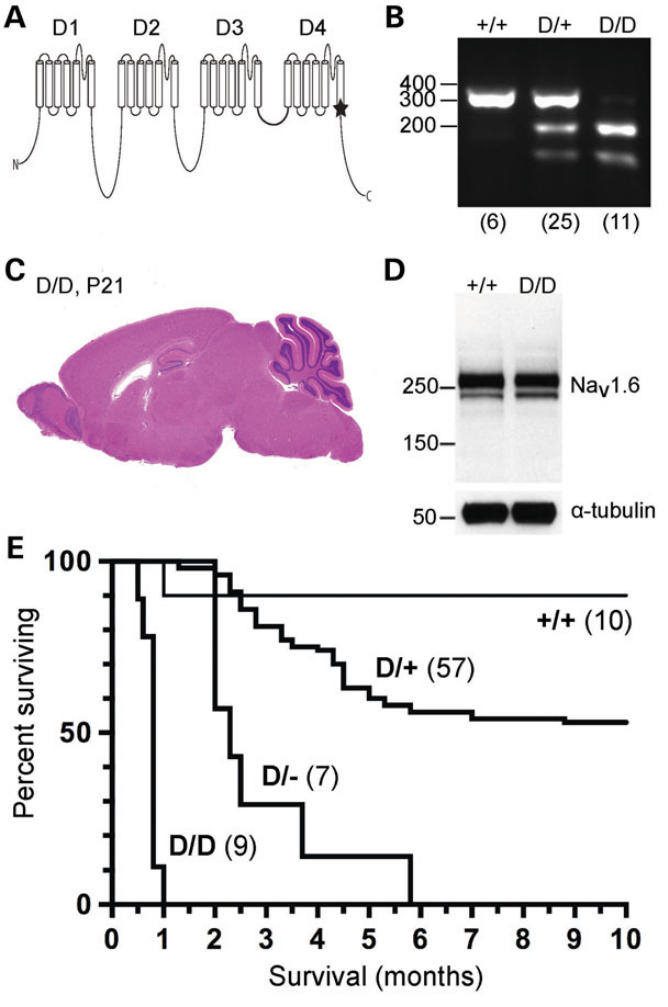

Figure 1. (**A**) The mutation p.Asn1768Asp in sodium channel $Na_v1.6$ is located at the cytoplasmic end of transmembrane segment D4S6 in domain 4 of the channel (star). (**B**) PCR/RFLP genotyping of heterozygous and homozygous mutants, using the introduced *Hinc*II site. The number of offspring with each genotype obtained by intercrossing D/+ heterozygotes is indicated below the lane. D/D and D/+ mice were obtained at frequencies consistent with the Mendelian prediction of 1:2:1 ($P = 0.25$). (**C**) Sagittal section of D/D brain at P21 with normal gross morphology. (**D**) Western blot of brain membrane protein (50 μg) from wild-type and homozygous mutant demonstrates comparable abundance of $Na_v1.6$ protein. (**E**) Survival of *Scn8a* mutant mice with genotypes D/D, D/+ and D/−. The number of mice of each genotype is indicated. The survival of wild-type littermates is shown.

The brief severe generalized tonic–clonic seizures in D/+ and D/D mice are usually <1 min in duration. Seizures begin with tonic hindlimb extension and limb clonus (Fig. 2A–C). Seizures are often followed by short periods of immobility and rapid breathing lasting 15–45 s. After the seizure, mice may recover quickly and regain normal mobility. Alternatively, prolonged behavioral arrest like that shown in Figure 2D may precede or follow a convulsive seizure. Episodes of ataxia and Straub tail are common after onset of seizures (Fig. 2E and F). Video recordings of representative seizures in D/+ and D/D mice are provided as Supplementary Material.

Table 1. Seizure onset and progression in mice carrying the Scn8a^{N1768D} mutation

Genotype	Preseizure phenotype	Age at seizure onset	Seizure progression	Terminal events	Median age at death (mean ± SD)	% with SUDEP
D/D	Tremor	3 weeks	No seizures prior to day of SUDEP	Sudden failure of motor function, multiple seizures within 24 h	3 weeks (3 ± 0.6)	100% (9/9)
D/−	Tremor ataxia	8 weeks	Multiple seizures per day	Impaired motor function, cluster of many seizures lasting ∼2 h	9 weeks (12 ± 6)	100% (7/7)
D/+	None	8–16 weeks	0–3 Seizures per day	Not observed	14 weeks (15 ± 7)	47% (27/57)

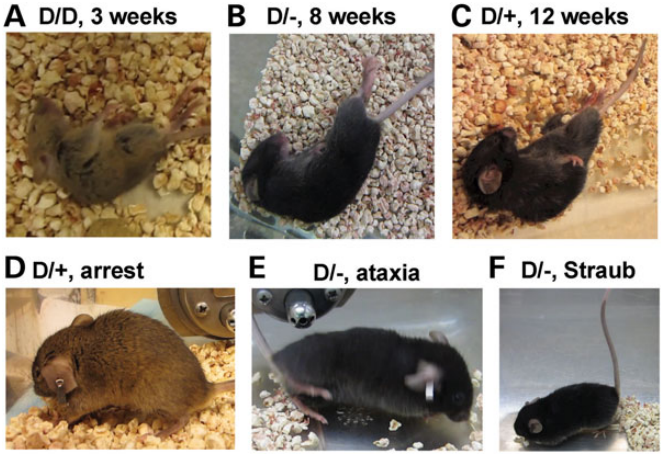

Figure 2. Seizure-associated behaviors in N1768D mutant mice. Severe generalized tonic–clonic seizures with hind limb extension in D/D, D/+ and D/− mice (**A**–**C**). Just before convulsive seizures, and between seizures, the mutant mice exhibit behavioral arrest lasting several minutes (**D**), sporadic loss of coordination with impaired gait (**E**), and Straub tail (**F**).

These data demonstrate that heterozygosity or homozygosity for the N1768D allele of *Scn8a* is sufficient to cause early onset of an epileptic encephalopathy-like syndrome in the mouse.

Normal abundance of $Na_v1.6$ protein in brain of homozygous D/D mice

Analysis of brain extracts from homozygous D/D mice at postnatal day 18 enabled us to assess the level of N1768D protein without the presence of wild-type channel. We carried out western blotting of brain membrane proteins followed by immunostaining to compare the abundance of $Na_v1.6$ in wild-type (+/+) and D/D brain. The intensity of immunostaining did not differ between +/+ and D/D samples (Fig. 1D). The N1768D mutation thus does not impair *in vivo* stability of the channel protein. This result is consistent with the model that the seizure phenotype is the result of the hyperactivity gain of function previously demonstrated in neurons transfected with the mutant channel (9).

Effects of dosage of mutant and wild-type Nav1.6

The earlier onset and increased mortality observed in D/D mice compared with D/+ mice could result from the double dose of the mutant allele and/or from the absence of a functional wild-type channel in the homozygous mutant. To separately evaluate these mechanisms, we generated D/− mice carrying a single copy of the mutant allele but lacking wild-type $Na_v1.6$. Heterozygous D/+ mice were crossed with +/− mice carrying the null allele *Scn8a*^{medtg} that does not produce $Na_v1.6$ protein due to an intragenic insertion (24,25). Offspring with the four predicted *Scn8a* genotypes were obtained in the predicted Mendelian ratio of 1:1:1:1 [+/+ (14), D/+ (12), +/− (10) and D/− (16) ($P = 0.67$)]. Analysis of the D/− mice revealed a less severe phenotype than D/D homozygotes, with later age of seizure onset (8 weeks for D/− compared with 3 weeks for D/D), slower progression (weeks rather than hours), and longer average survival (3 months for D/− compared with 3 weeks for D/D) (Fig. 1E and Table 1). Thus, in the absence of wild-type $Na_v1.6$, two copies of the mutant allele in D/D mice are more deleterious than the single copy in D/− mice, demonstrating a direct correlation between dosage of the mutant allele and severity.

The phenotype of D/− mice includes fine tremor and mild gait impairment, and is more severe than D/+ mice. D/− mice exhibit as many as 25 seizures in a single day compared with 0–3 seizures per day in D/+ mice (Table 1). D/− mice exhibit clusters of generalized tonic–clonic seizures with progressively shorter latency between seizures. Seizures are followed by rapid breathing or gasping eventually leading to cessation of breathing. In three D/− mice we observed death that occurred after a cluster of 18–25 seizures. The appearance of respiratory distress in the mice is reminiscent of the events leading to terminal apnea in the MORTEMUS study of epilepsy patients with SUDEP (26). The later onset and reduced seizure frequency in D/+ mice compared with D/− mice demonstrates that protection is conferred by the presence of the wild-type $Na_v1.6$ channel (Table 1).

Abnormal EEG activity accompanies behavioral seizures in *Scn8a* mutant mice

D/+ and D/− mice were assessed by video/EEG monitoring between 6 and 10 weeks of age. Wild-type controls were recorded simultaneously. Overt EEG abnormalities were not observed earlier than 7 weeks of age. At 7 weeks, semiperiodic large biphasic slow wave or sharp wave–slow wave complexes were observed in all leads. In D/+ mice these discharges occurred sporadically and were occasionally associated with myoclonic jerks (<5%). In the D/− mouse, discharges were usually accompanied by behavioral myoclonic jerks, typically involving the hindlimbs, with a frequency of 1–2 per hour, or by more generalized spasms. These abnormalities were never seen in wild-type mice. D/+ and D/− mice also exhibited

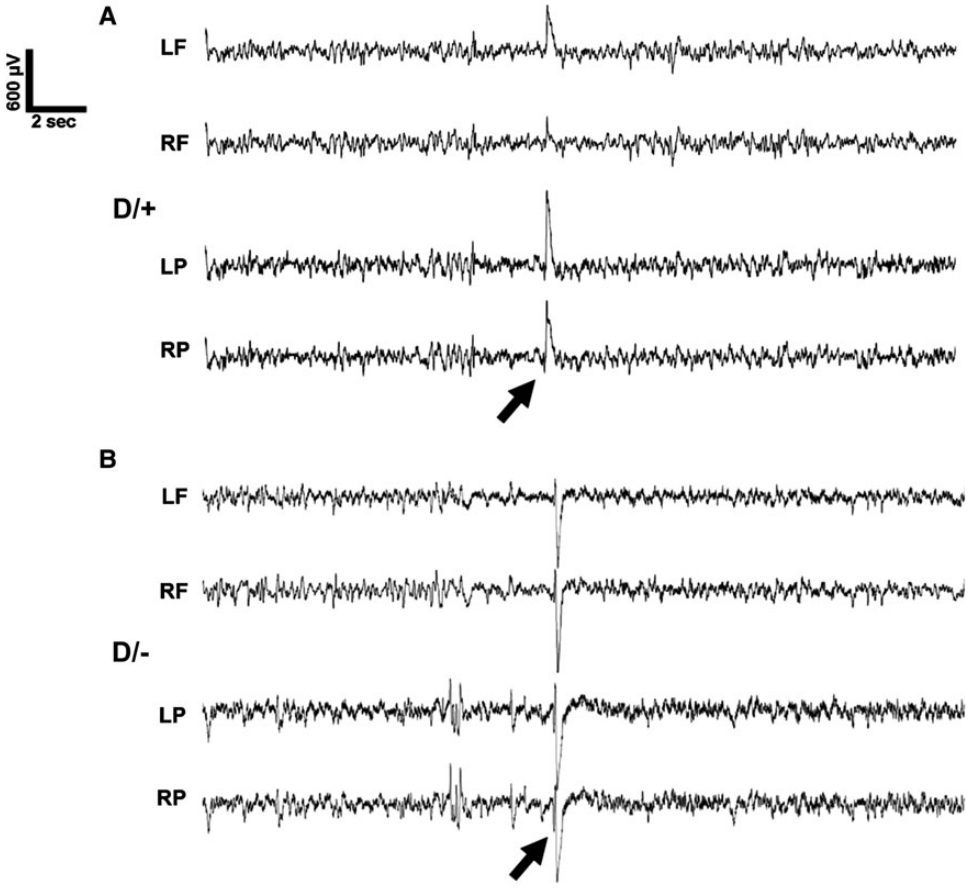

Figure 3. Interictal EEG recordings from *Scn8a* mutant mice. Epileptiform discharges were observed in D/+ and D/− mice (arrows). Spike, sharp wave or spike-wave discharges were observed in all leads and were often associated with myoclonic jerks. Wild-type mice did not exhibit these waveforms. LF and RF, left and right frontal; LP and RP, left and right parietal.

multiple daily interictal epileptiform discharges consisting of diffuse polyspikes or single spike-wave discharges that were frequently accompanied by myoclonic jerks (Fig. 3).

Both D/+ and D/− mice experienced periods of behavioral arrest and repetitive grooming that were not associated with a consistent EEG correlate. Each mutant genotype experienced convulsive seizures associated with ictal electrographic patterns that were characterized by high-amplitude sharp wave–slow wave activity followed by diffuse suppression and a buildup of paroxysmal high-amplitude fast activity (Fig. 4A–C). The seizures continued with repetitive spike-and-wave activity that transitioned to low-amplitude theta activity. Behaviorally the mice displayed clonic jerking at the onset of the electrographic seizure, followed by tonic activity associated with the Straub tail phenomenon (see example in Fig. 2F). Repetitive movements of the hindlimbs were common. Postictal changes consisted of continuous theta waves interspersed with intermittent periods of normal activity, large spike-wave discharges and extended periods of EEG suppression for up to 20 min before the return of normal background activity. The frequency of these larger convulsive seizures varied with genotype. The D/+ mouse whose EEG recording is shown in Figure 4B had two seizures separated by 7 days. The D/− mouse (Fig. 4C) had a cluster of three seizures in a 48 h period, and no further seizures were captured during 30 days of recording. No seizures were observed in the wild-type controls.

Most animals were recorded from surface electrodes. In a subset of D/+ mice, however, we used both surface and depth electrodes placed in the amygdala and hippocampus to explore whether seizures originated focally in either of these regions. We found no evidence of localized onset as ictal discharges appeared nearly simultaneously in all electrodes (Fig. 4B).

Motor learning and open field behavior

The proband carrying the N1768D mutation experienced ataxia as well as impaired coordination and balance (9). Visibly impaired gait was evident in the D/D and D/− mutant mice, but the gait of D/+ mice appeared normal. To further evaluate the motor function of D/+ mice, we examined motor learning and coordination in mice that had not exhibited visible seizures. The accelerating rotarod test was employed. On the first trial, D/+ mice maintained their position on the rotarod for only 50% the length of time of +/+ mice (Fig. 5A). During training, both +/+ and D/+ mice exhibited motor learning, but the mutant mice never achieved the wild-type performance level (Fig. 5A), indicating an intrinsic impairment of motor function. To determine whether the performance deficit on the rotarod

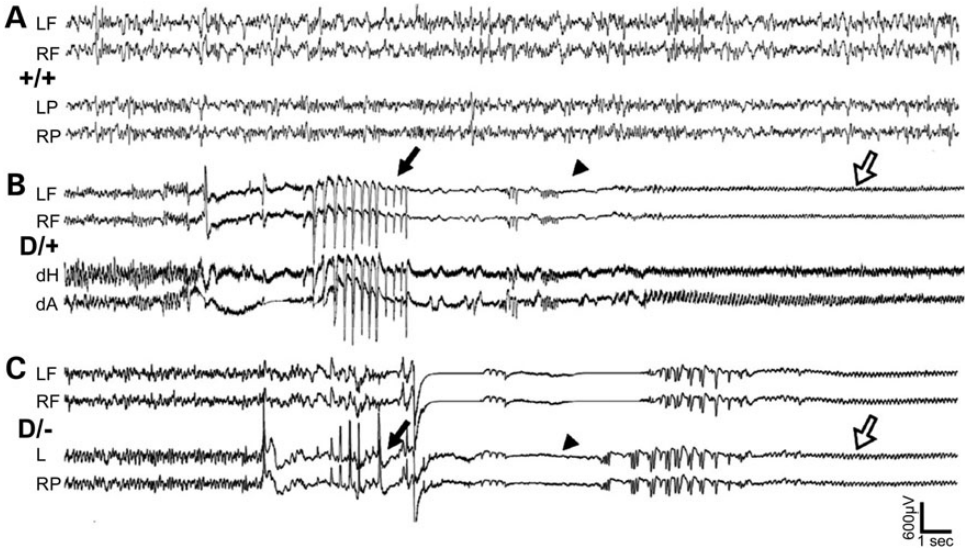

Figure 4. EEG during spontaneous seizures in *Scn8a* mutant mice. (**A**) Representative EEG epoch of a wild-type (+/+) mouse. (**B** and **C**) Electrographic seizures recorded from D/+ mice (B) and D/− mice (C) demonstrate a similar evolution of sharp wave activity (arrows) and suppression (arrowheads), followed by low-amplitude theta activity (open arrows). LFF 1 Hz, HFF 70 Hz, NF 60 Hz, 30 μV/mm, PS 15 mm/s. LF and RF, left and right frontal; LP and RP, left and right parietal; dH and dA, hippocampal and amygdala depth electrodes.

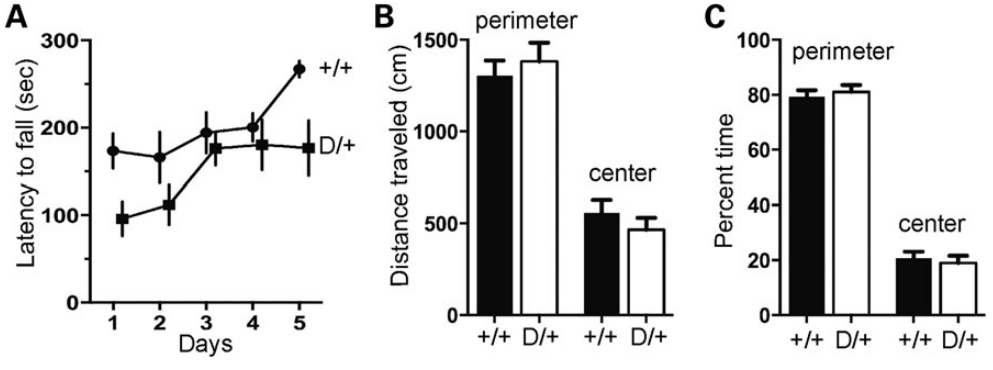

Figure 5. Motor coordination and open field behavior of heterozygous N1768D (D/+) mice. (**A**) Impaired motor coordination on the accelerating rotarod. Each mouse was given a 5 min trial on five consecutive days. +/+, $n = 9$; D/+, $n = 9$. (**B**) Total distance traveled by D/+ mice ($n = 9$) in the open field behavior test was not significantly different from +/+ mice ($n = 9$). (**C**) The percent of time spent in the center of the open field by D/+ mice was not significantly different from +/+ mice.

resulted from motor weakness, we assessed grip strength and performance in the wire-hang test. The grip force of D/+ mice was 118 ± 7 g ($n = 5$), which did not differ from the wild-type value of 123 ± 6 g ($n = 3$). Both D/+ mice ($n = 3$) and +/+ mice ($n = 3$) were able to hang from the wire mesh for the full 60 s trial period. These results indicate that the rotarod performance deficit of D/+ mice does not result from muscle weakness, but rather from impaired coordination.

In the open field test, D/+ mice did not differ from +/+ mice with respect to total distance covered or percent of time spent in the open center area (Fig. 5B and C). These data indicate that D/+ mice do not exhibit elevated anxiety, in distinction from our previous report on haploinsufficient *Scn8a*$^{+/-}$ mice (27).

Fear conditioning

We assessed associative learning and memory by Pavlovian fear conditioning using the protocol described in Materials and Methods. On Day 1, before the first exposure to a paired tone and shock, there was no freezing behavior in the treatment cage by D/+ ($n = 7$) or wild-type ($n = 9$) mice (Fig. 6A). On Day 2 and Day 3, after training by exposure to paired tone and shock, mice of both genotypes demonstrated a comparable increase in freezing behavior in the context of the test cage (Fig. 6A). When exposed to the context of the test cage in the absence of tone on Day 4, +/+ and D/+ mice spent equivalent time in freezing behavior (Fig. 6B). On Day 5, in the cued conditioning test, both +/+ and D/+ mice exhibited significantly more freezing after exposure to the tone ($P < 0.0001$) (Fig. 6C). These data indicate that prior to the onset of seizures, D/+ mice do not have a deficit in associative learning or memory.

Social interaction

The proband carrying the N1768D mutation exhibited reduced social interaction and was diagnosed with autistic features at 5

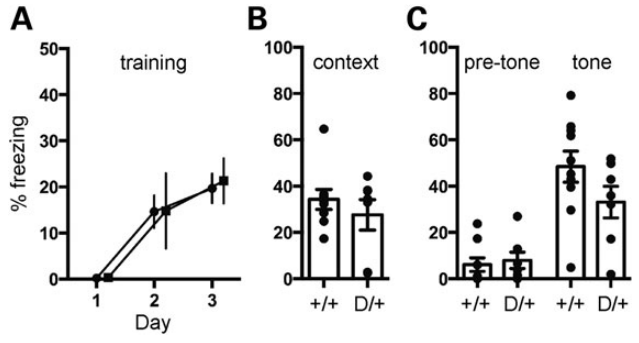

Figure 6. Fear-conditioning behavior of heterozygous N1768D (D/+) mice. (**A**) Normal learning during a 3-day fear-conditioning protocol. +/+ (circle), $n = 9$; D/+ (square), $n = 7$. (**B**) Normal freezing to context on Day 4 of fear conditioning. (**C**) Normal freezing in response to the cued stimulus (tone).

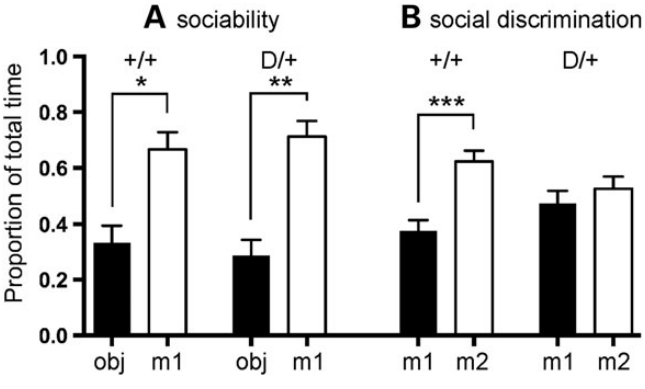

Figure 7. Social interaction behavior of heterozygous N1768D (D/+) mice. (**A**) Sociability. D/+ mice exhibit normal preference for a novel mouse (m1) rather than an inanimate object (obj) in the three-chamber social interaction task. +/+, $n = 9$; D/+, $n = 7$ ($^{*}P = 0.03$, $^{**}P = 0.005$). (**B**) Social discrimination. The D/+ mutant failed to discriminate between the now-familiar mouse (m1) and a novel mouse (m2) in the three-chamber social interaction test ($^{*}P = 0.01$).

years of age (9). To determine whether D/+ mice reflect this aspect of the disorder, we used the three-chambered social interaction test to assess sociability and preference for social novelty. We initially compared the time spent sniffing a novel animal to the time spent sniffing a novel inanimate object. Both D/+ and +/+ mice exhibited preference for the novel animal, m1, consistent with normal sociability (Fig. 7A). In the second test, we compared the time spent sniffing the original animal, now familiar, with the time spent sniffing an unfamiliar mouse. Wild-type mice spent significantly more time with the unfamiliar mouse (m2), indicating a preference for social novelty (Fig. 7B). The D/+ mice spent equal time sniffing the familiar and the unfamiliar mouse (Fig. 7B), suggesting an impairment in social discrimination.

The deficient performance in the social novelty test could be influenced by impaired cognition or impaired olfaction. To detect impaired olfaction, we evaluated the ability of D/+ mice to detect buried food. The time required to detect the buried food was 50 ± 14 s for the D/+ mice ($n = 7$) and 53 ± 9 s for the wild-type mice ($n = 9$) (mean ± SEM, $P = 0.84$), indicating that there is no olfactory deficit in the D/+ mice.

DISCUSSION

SCN8A^{N1768D} was identified as a *de novo* heterozygous mutation in a proband with epileptic encephalopathy (9). Since *de novo* mutations arise on a genetic background that includes many rare variants, it is difficult to distinguish between the direct effects of the mutation and the modifier contributions of inherited variants. Introduction of the *Scn8a*^{N1768D} mutation into the mouse genome has generated a disease model that reproduces several key aspects of the human disorder, including generalized seizures, epileptiform events on EEG, impaired motor coordination and SUDEP, confirming the causal role of the *de novo* *SCN8A* mutation in these aspects of the disorder.

In the proband with the gain-of-function mutation in *SCN8A*, seizure onset was at 6 months of age, with brief generalized seizures and synchronous clonic jerks of the arms and hands (9). After learning to walk at 3 years of age, the proband exhibited ataxia, hypotonia and occasional unresponsiveness similar to the episodes of loss of motor control in the D/D and D/− mice; these unusual features may be characteristic of *Scn8a* dysfunction. At 4.5 years she began to experience epileptic spasms that persisted until SUDEP at the age of 15 years (9). The frequency of daytime seizures varied from 1 per week to 4 per week with typical duration of 1–20 min. The response of patients with different types of sodium channel mutations to treatment with sodium channel blockers is an important issue for epilepsy management. In the case of the proband, valproate monotherapy was started after the initial seizures and reduced but did not completely eliminate seizures. With the addition of lamotrigine, seizures were well controlled until the start of epileptic spasms. Improved but incomplete control was achieved with the addition of clobazam. Both valproate and lamotrigine act at least in part as sodium channel blockers, suggesting that these types of AEDs may be useful for some epileptic encephalopathies caused by gain-of-function sodium channel mutations. The *Scn8a*^{N1768D} knock-in mouse will be a valuable model for evaluation of treatments for this class of epileptic encephalopathy, including drugs that specifically target the persistent current that is elevated by this mutation.

In comparison to the mutant mice, the onset of seizures in the proband was closer in developmental stage to the D/D homozygote, but progression was slower and more closely resembled the D/+ mice. By generating a 'functionally hemizygous' mouse with genotype D/−, we were able to demonstrate that two factors contribute to greater severity of D/D homozygotes. First, there is a deleterious effect of the extra copy of the mutant channel, as demonstrated by the comparison of D/D and D/− mice (Table 1). Second, the protective effect of the wild-type channel is demonstrated by the reduced disease severity in D/+ compared with D/− mice (Table 1). The severity of epileptogenesis may be determined by the abundance of the mutant channel in the axon initial segment (AIS) where action potentials are initiated. During postnatal mouse development, the AIS is first occupied by the $Na_v1.2$ channel, which is gradually displaced by $Na_v1.6$ between 2 and 3 weeks of age (17,28,29). The predominance of $Na_v1.2$ at the AIS up to 2 weeks of age may explain the normal phenotype of D/D mice during the first 2 weeks of life. Similarly, the movement disorder in $Na_v1.6$ null mice begins at 2 weeks of age (24,30). The later onset of seizures in D/− mice at 2 months compared with 3 weeks for D/D mice, may

result from delayed maturation of the AIS due to the reduced expression of $Na_v1.6$ from a single gene copy. In D/+ mice, competition by wild-type $Na_v1.6$ may reduce the abundance of mutant channel at the AIS, resulting in later seizure onset and progression than in D/− mice. Nav1.6 is present in interneurons as well as excitatory neurons (12), yet the overall effect of this gain-of-function mutation is hyperexcitability, suggesting a greater impact in excitatory neurons. This may reflect the different channel expression profile in these cells, or the complexity of distributed and local neuronal networks and their synchronization. Future analysis of mice with conditional expression of the mutant in each type of neuron could address the impact on each directly.

The electrographic seizure and behavioral activity of *Scn8a*$^{N1768D/+}$ mice shared several key features with that of the patient carrying this mutation (9). The patient exhibited brief epileptic spasms and tonic seizures with electrographic correlates, as did the mice. The subject and the mouse model both displayed frequent interictal spikes as well as ictal patterns consisting of high-amplitude discharges followed by background suppression. The patient experienced SUDEP, and this was a frequent complication in the mouse model. Thus, *Scn8a* mutant mice model the clinical and electrographic seizure phenotype associated with the human *SCN8A* mutation.

Encephalopathy is an important component of the human disorder, and is characterized by developmental delay and cognitive impairment. To determine whether the mouse model recapitulates this aspect of the disorder, further testing to evaluate discriminative and spatial learning will be required. It will be especially interesting to compare these functions before and after the onset of seizures. The normal function of D/+ mice in fear-conditioning tests demonstrates that D/+ mice retain a basic level of cognition and memory prior to seizure onset. We identified minor deficits in tests of motor coordination and social discrimination; the latter might be accounted for by a cognitive deficit.

The epileptogenic effect of the gain-of-function N1768D mutation on *SCN8A* is different from the effect of loss-of-function mutations. Although haploinsufficiency of *SCN1A* results in spontaneous seizures in human (Dravet Syndrome) and mouse, haploinsufficiency of *SCN8A* does not always lead to spontaneous seizures in either species (12). Haploinsufficiency of both *SCN1A* and *SCN8A* can impair cognition in the absence of seizures. For example, conditional inactivation of *Scn1a* that was restricted to forebrain neurons resulted in learning impairment without seizures in rats (31) and mice (32), and haploinsufficiency of *SCN8A* led to cognitive impairment in a human family with no history of epilepsy (33).

The N1768D mutant is the first mouse model with a gain-of-function mutation of *Scn8a*. Homozygosity for previously studied *Scn8a* alleles with partial- or complete- loss-of-function results in movement disorders (11). The severity of these disorders is proportional to the extent of $Na_v1.6$ deficiency. Loss of 90% of $Na_v1.6$ protein results in chronic dystonia (34,35), while loss of 100% of protein leads to paralysis and juvenile lethality (24). A depolarizing shift in voltage dependence of activation of $Na_v1.6$, which is opposite in effect to the N1768D mutation, results in recessively inherited ataxia (25,36). None of the loss-of-function alleles result in spontaneous seizures even in homozygous animals, and *Scn8a*$^{+/-}$ haploinsufficient mice are more resistant to seizure induction by electrical, chemical and genetic causes (37–39). These data are consistent with the role of $Na_v1.6$ in initiation of action potentials at the axon initial segment and support the view that hyperactivity of $Na_v1.6$ is epileptogenic while hypoactivity can be protective. Gain-of-function in a second epileptogenic mutation of *SCN8A* is consistent with this model (11). However, loss-of-function of $Na_v1.6$ may contribute to seizure susceptibility in certain genetic contexts. Thus, on certain strain backgrounds, haploinsufficient *Scn8a*$^{+/-}$ mice exhibit spontaneous spike-wave discharges (40). These considerations demonstrate the importance of functional evaluation of newly identified *SCN8A* mutations to clarify underlying pathogenic mechanisms and aid in developing rational antiepileptic therapies.

In summary, we have developed a novel knock-in mouse model of human epileptic encephalopathy caused by a dominant, gain-of-function missense mutation in *Scn8a.* The *Scn8a*^{N1768D} mouse will be valuable for further delineation of the molecular and physiological consequences of $Na_v1.6$ hyperactivity, the pathogenesis of epileptic encephalopathy, and the response to therapeutic interventions.

MATERIALS AND METHODS

Animals

The *Scn8a*^{N1768D} knock-in allele was generated by TALEN targeting of (C57BL/6JXSJL)F2 eggs at the University of Michigan Transgenic Animal Model Core as previously described (23). The line was propagated by backcrossing N1768D/+ heterozygotes to C57BL/6J wild-type mice (The Jackson Laboratory, Bar Harbor, ME). Mice were housed and cared for in accordance with NIH guidelines. Experiments were approved by the University of Michigan Committee on the Use and Care of Animals. Mice used for behavioral experiments were from the N3 generation. Compound heterozygous mice carrying one N1768D allele and one null allele were generated by crossing *Scn8a*$^{N1768D/+}$ mice to heterozygous congenic B6.medtg mice carrying the null allele *Scn8a*^{medtg} on strain C57BL/6J (24).

Genotyping

DNA was isolated from tail biopsies by digestion with 1 μg/μl proteinase K in buffer containing 50 mM KCl, 10 mM Tris–HCl pH8.0, and 0.1% Triton X-100. Genotyping was performed as previously described, using the introduced *Hinc*II site in the mutant allele (23). A 327 bp genomic fragment of *Scn8a* containing the mutation was amplified by PCR with the primers Tar-F [5′-TGACT GCAGC TTGGA CAAGG AGC-3′) and Tar-R (5′-TCGAT GGTGT TGGGC TTGGG TAC-3′]. PCR products were digested with *Hinc*II and analyzed on a 2% agarose gel stained with ethidium bromide. The wild-type allele generates a single fragment of 327 bp and the mutant allele generates two fragments of 209 and 118 bp.

Western blotting

Membrane proteins were isolated from whole brain as previously described (41). Briefly, brain tissue from mice at postnatal day 18 (P18) was homogenized and centrifuged at 3500 *g* for 10 min, and membrane proteins were pelleted from the supernatant at

100 000 *g* for 30 min. Protein concentration was measured with the BCA assay (Thermo-Fisher, Waltham, MA). Samples containing 50 μg of protein were incubated at 37°C for 20 min in sample loading buffer prior to electrophoresis on 4–15% gradient SDS-PAGE gels (Bio-Rad, Hercules, CA). After transfer, filters were cut and incubated with polyclonal antibody to $Na_v1.6$ (ASC-009, 1:100; Alomone Labs, Jerusalem, Israel), or with monoclonal antibody to α-tubulin (CLT9002, 1:1000, Cedarlane Labs, Burlington, Canada) as a loading control.

Histology

The brain was removed from a P21 N1768D/N1768D homozygote and immersion fixed for 24 h at 4°C in phosphate-buffered 10% formalin and then in 70% ethanol for an additional 24 h at 4°C. Paraffin embedding and Hematoxylin and eosin staining were carried out at Histoserv Inc. (Bethesda, MD).

Video/EEG monitoring

Animals were kept under a constant 12 h light/dark cycle with access to food and water *ad libitum.* Procedures for affixing subdural electrodes were performed as previously described (42,43). Mice were anesthetized with a ketamine/xylazine mixture and placed in a stereotaxic mouse adaptor (Stoelting, Wood Dale, IL). Six holes were made into the skull using a #56 gauge steel bit. Electrodes were positioned and fastened (left and right frontal, left and right parietal, one cerebellar and one reference over the sinus cavity) using mounting screws (E363/20; PlasticsOne, Roanoke, VA). For the acquisition of local field potentials, the left and right parietal electrodes were replaced with multichannel depth electrodes (E363/1/SPC; PlasticsOne, Roanoke, VA). Each depth electrode was stereotactically positioned, one in the left hippocampus (AP −2.0, ML 1.6, DV −1.5) and one in the right amygdala (AP −1.2, ML 3.0, DV −4.5). The sockets were fitted into a 6-pin electrode pedestal and the entire apparatus was secured with dental cement (Stoelting). Animals received buprenorphine subcutaneously for three days and then were monitored for up to 30 days, in 10 day increments, by continuous video/EEG recording (Ceegraph Vision; Bio-logic System Corporation). Recordings were sampled at 256 Hz and concurrent video was analyzed offline and synced with EEG data. Seizures and epileptiform activity were assessed manually by an observer blinded to the genotypes. Interictal epileptiform discharges (IEDs) were defined as paroxysmal activity, distinct from background, and consisting of waveforms lasting 20–200 ms. Seizures were categorized into two groups: (i) myoclonic jerk-like events identified as high-amplitude (> 700 microvolts) spike-wave, sharp wave-slow wave or biphasic slow wave discharges seen in all leads and associated with brief paroxysmal motor behavior; (ii) more complex convulsive events associated with paroxysmally appearing rhythmic waveforms (slow waves, sharp waves or high-amplitude theta activity) that persisted for a minimum of 10 s and displayed an unequivocal evolution in frequency and morphology, followed by postictal alterations prior to recovery of baseline activity.

Behavioral assessment of *Scn8a*$^{N1768D/+}$ mice

D/+ heterozygotes ($n = 9$) and wild-type littermates ($n = 9$) were used for behavioral testing beginning at 8 weeks of age. Behavioral tests were carried out in the following order: social interaction, open field, rotarod and fear conditioning. Behavioral testing was carried out blind to genotype.

Accelerating rotarod

Assessment of motor coordination and motor learning was performed as previously described (27). Wild-type ($n = 9$) and D/+ ($n = 7$) mice were placed on the rotating drum of an accelerating rotarod (Ugo Basile, Comerio, Italy). Rotation was accelerated from 4 to 40 rpm during the test period of 5 min. Mice were given one trial per day on five successive days. Latency to fall or to first passive rotation was recorded. Experimenters were blind to genotype throughout the testing.

Grip strength

Grip strength was measured using a grip strength meter (Chatillon E-DFE-002; Columbus, OH) with a metallic grid (12 × 10 cm). Mice were held by the tail and lowered over the center of the grid to permit grasping by forelimbs and hindlimbs. With the body parallel to the grid, the mouse was pulled steadily backward until grip was released. The lateral force (grip force) exerted on the gauge at the time of release was recorded as peak tension (grams of force). Assays were repeated three times each day for four consecutive days; mean values for each animal were calculated from the 12 measurements.

Open field

Assessment of mouse behavior in an open field was performed as previously described (27). Individual mice ($n = 9$ for each genotype) were placed at the center of a white acrylic chamber (71 × 71 × 30 cm) lit by indirect white light (200 lux at center of chamber) and allowed to explore for 5 min. The open field was divided into an 8 × 8 grid with a center zone (53.25 × 53.25 cm) and a peripheral zone (the outer 8.875 cm on all sides). Total distance traveled in the center zone was measured by video signals from digital cameras sent to a desktop PC and processed online with Actimetrics LIMELIGHT software. Experimenters were blind to genotype throughout.

Pavlovian fear conditioning

The Pavlovian fear-conditioning apparatus (Med Associates Inc., St. Albans, VT) was previously described (27). Fear was assessed by measuring freezing behavior, defined as the absence of movement except that associated with respiration, and was measured by subjecting the video signal to a sensitive global motion detection algorithm (FREEZEFRAME version 2.04 and FREEZEVIEW version 2.1 software; Actimetrics, Wilmette, IL). Data are presented as percent freezing, the amount of time an individual animal spent freezing divided by the duration of the trial and multiplied by 100. Wild-type mice ($n = 9$) and D/+ mice ($n = 7$) received three training trials (one per day) in which a 3 min baseline was followed by a 30 s tone that co-terminated with a 2 s, 0.75 mA foot shock delivered through the grid floor. Mice were removed from the chambers after an additional 80 s. Twenty-four hours after the last training trial, on Day 4, context conditioning was assayed by returning

mice to the chambers and assessing freezing during a 5 min trial in the absence of tone or shock. On Day 5, cued conditioning was assessed by measurement of response to a 3 min tone in the conditioning chambers that were reconfigured as described (27). Experimenters were blind to genotype throughout the testing.

Social interaction

Evaluation of sociability and preference for social novelty was performed using a three-chamber social interaction test (44). Wild-type ($n = 9$) and D/+ ($n = 9$) mice (male and female) were habituated to the three-chambered arena for 10 min on Day 1. On Day 2, each experimental mouse was habituated again for 5 min and then placed in a holding cage. To test for sociability, an empty woven metal container was placed in one of the side chambers, and an unfamiliar mouse was placed under a woven metal container in the other side chamber. The unfamiliar mouse was a naïve, 2–3-month-old C57BL/6J mouse of the same sex as the experimental mouse. The experimental mouse was placed in the center chamber that was open to both sides and allowed to explore for 5 min. To test for preference for social novelty, the experimental mouse was again placed in a holding cage while a different unfamiliar mouse with the characteristics described above was placed under the empty woven metal container. The experimental mouse was placed in the center chamber that was open to both sides and allowed to explore for 5 min. Video signals from digital cameras were sent to a desktop PC and processed online with Actimetrics LIMELIGHT software. The videos were scored by an observer blind to genotype. Time spent in each chamber and time spent sniffing the empty woven metal container or the mice in the containers was recorded.

NOTE ADDED IN PROOF

Two *de novo* loss-of-function mutations in *SCN8A* have recently been described (45, 46).

SUPPLEMENTARY MATERIAL

Supplementary Material is available at *HMG* online.

ACKNOWLEDGEMENTS

We thank Margaret Wu for genotyping, Jonathan Chuko for measurement of grip strength and H. Stason Schafer for assistance with behavioral tests.

Conflict of Interest statement. None declared.

FUNDING

This work was supported by the National Institutes of Health (NS34509 to M.H.M., NS58585 to J.M.P.). Funding to pay the Open Access publication charges for this article was provided by the National Institutes of Health Grant NS34509 to M.H.M.

REFERENCES

1. Berg, A.T., Berkovic, S.F., Brodie, M.J., Buchhalter, J., Cross, J.H., van Emde Boas, W., Engel, J., French, J., Glauser, T.A., Mathern, G.W. *et al.* (2010) Revised terminology and concepts for organization of seizures and epilepsies: report of the ILAE Commission on Classification and Terminology, 2005–2009. *Epilepsia*, **51**, 676–685.
2. Carvill, G.L., Heavin, S.B., Yendle, S.C., McMahon, J.M., O'Roak, B.J., Cook, J., Khan, A., Dorschner, M.O., Weaver, M., Calvert, S. *et al.* (2013) Targeted resequencing in epileptic encephalopathies identifies de novo mutations in CHD2 and SYNGAP1. *Nat. Genet.*, **45**, 825–830.
3. Epi4K Consortium; Epilepsy Phenome/Genome Project; Allen, A.S., Berkovic, S.F., Cossette, P., Delanty, N., Dlugos, D., Eichler, E.E., Epstein, M.P., Glauser, T., Goldstein, D.B., Han, Y. *et al.* (2013) De novo mutations in epileptic encephalopathies. *Nature*, **501**, 217–221.
4. Kodera, H., Kato, M., Nord, A.S., Walsh, T., Lee, M., Yamanaka, G., Tohyama, J., Nakamura, K., Nakagawa, E., Ikeda, T. *et al.* (2013) Targeted capture and sequencing for detection of mutations causing early onset epileptic encephalopathy. *Epilepsia*, **54**, 1262–1269.
5. Veeramah, K.R., Johnstone, L., Karafet, T.M., Wolf, D., Sprissler, R., Salogiannis, J., Barth-Maron, A., Greenberg, M.E., Stuhlmann, T., Weinert, S. *et al.* (2013) Exome sequencing reveals new causal mutations in children with epileptic encephalopathies. *Epilepsia*, **54**, 1270–1281.
6. Mastrangelo, M. and Leuzzi, V. (2012) Genes of early-onset epileptic encephalopathies: from genotype to phenotype. *Pediatr. Neurol.*, **46**, 24–31.
7. Nicita, F., De Liso, P., Danti, F.R., Papetti, L., Ursitti, F., Castronovo, A., Allemand, F., Gennaro, E., Zara, F., Striano, P. *et al.* (2012) The genetics of monogenic idiopathic epilepsies and epileptic encephalopathies. *Seizure*, **21**, 3–11.
8. Meisler, M.H., O'Brien, J.E. and Sharkey, L.M. (2010) Sodium channel gene family: epilepsy mutations, gene interactions and modifier effects. *J. Physiol.*, **588**, 1841–1848.
9. Veeramah, K.R., O'Brien, J.E., Meisler, M.H., Cheng, X., Dib-Hajj, S.D., Waxman, S.G., Talwar, D., Girirajan, S., Eichler, E.E., Restifo, L.L. *et al.* (2012) De novo pathogenic SCN8A mutation identified by whole-genome sequencing of a family quartet affected by infantile epileptic encephalopathy and SUDEP. *Am. J. Hum. Genet.*, **90**, 502–510.
10. Dyment, D.A., Tetreault, M., Beaulieu, C.L., Hartley, T., Ferreira, P., Warman Chardon, J., Marcadier, J., Sawyer, S.L., Mosca, S.J., Micheil Innes, A. *et al.* (2014) Whole-exome sequencing broadens the phenotypic spectrum of rare pediatric epilepsy: a retrospective study. *Clin. Genet.*, doi: 10.1111/cge.12464.
11. Estacion, M., O'Brien, J.E., Conravey, A., Hammer, M.F., Waxman, S.G., Dib-Hajj, S.D. and Meisler, M.H. (2014) A novel de novo mutation of SCN8A (Na1.6) with enhanced channel activation in a child with epileptic encephalopathy. *Neurobiol. Dis.*, **69C**, 117–123.
12. O'Brien, J.E. and Meisler, M.H. (2013) Sodium channel SCN8A (Nav1.6): properties and de novo mutations in epileptic encephalopathy and intellectual disability. *Front. Genet.*, **4**, 213.
13. Ohba, C., Kato, M., Takahashi, S., Lerman-Sagie, T., Lev, D., Terashima, H., Kubota, M., Kawawaki, H., Matsufuji, M., Kojima, Y. *et al.* (2014) Early onset epileptic encephalopathy caused by de novo SCN8A mutations. *Epilepsia*, **55**, 994–1000.
14. Rauch, A., Wieczorek, D., Graf, E., Wieland, T., Endele, S., Schwarzmayr, T., Albrecht, B., Bartholdi, D., Beygo, J., Di Donato, N. *et al.* (2012) Range of genetic mutations associated with severe non-syndromic sporadic intellectual disability: an exome sequencing study. *Lancet*, **380**, 1674–1682.
15. Vaher, U., Noukas, M., Nikopensius, T., Kals, M., Annilo, T., Nelis, M., Ounap, K., Reimand, T., Talvik, I., Ilves, P. *et al.* (2013) De Novo SCN8A Mutation identified by whole-exome sequencing in a boy with neonatal epileptic encephalopathy, multiple congenital anomalies, and movement disorders. *J. Child. Neurol.*, doi:10.1177/0883073813511300.
16. Boiko, T., Rasband, M.N., Levinson, S.R., Caldwell, J.H., Mandel, G., Trimmer, J.S. and Matthews, G. (2001) Compact myelin dictates the differential targeting of two sodium channel isoforms in the same axon. *Neuron*, **30**, 91–104.
17. Boiko, T., Van Wart, A., Caldwell, J.H., Levinson, S.R., Trimmer, J.S. and Matthews, G. (2003) Functional specialization of the axon initial segment by isoform-specific sodium channel targeting. *J. Neurosci.*, **23**, 2306–2313.
18. Caldwell, J.H., Schaller, K.L., Lasher, R.S., Peles, E. and Levinson, S.R. (2000) Sodium channel Na(v)1.6 is localized at nodes of ranvier, dendrites, and synapses. *Proc. Natl. Acad. Sci. USA*, **97**, 5616–5620.
19. Krzemien, D.M., Schaller, K.L., Levinson, S.R. and Caldwell, J.H. (2000) Immunolocalization of sodium channel isoform NaCh6 in the nervous system. *J. Comp. Neurol.*, **420**, 70–83.
20. Hu, W., Tian, C., Li, T., Yang, M., Hou, H. and Shu, Y. (2009) Distinct contributions of Na(v)1.6 and Na(v)1.2 in action potential initiation and backpropagation. *Nat. Neurosci.*, **12**, 996–1002.

21. Lorincz, A. and Nusser, Z. (2008) Cell-type-dependent molecular composition of the axon initial segment. *J. Neurosci.*, **28**, 14329–14340.
22. Van Wart, A., Trimmer, J.S. and Matthews, G. (2007) Polarized distribution of ion channels within microdomains of the axon initial segment. *J. Comp. Neurol.*, **500**, 339–352.
23. Jones, J.M. and Meisler, M.H. (2014) Modeling human epilepsy by TALEN targeting of mouse sodium channel Scn8a. *Genesis*, **52**, 141–148.
24. Burgess, D.L., Kohrman, D.C., Galt, J., Plummer, N.W., Jones, J.M., Spear, B. and Meisler, M.H. (1995) Mutation of a new sodium channel gene, Scn8a, in the mouse mutant 'motor endplate disease'. *Nat. Genet.*, **10**, 461–465.
25. Sharkey, L.M., Cheng, X., Drews, V., Buchner, D.A., Jones, J.M., Justice, M.J., Waxman, S.G., Dib-Hajj, S.D. and Meisler, M.H. (2009) The ataxia3 mutation in the N-terminal cytoplasmic domain of sodium channel Na(v)1.6 disrupts intracellular trafficking. *J. Neurosci.*, **29**, 2733–2741.
26. Ryvlin, P., Nashef, L., Lhatoo, S.D., Bateman, L.M., Bird, J., Bleasel, A., Boon, P., Crespel, A., Dworetzky, B.A., Hogenhaven, H. *et al.* (2013) Incidence and mechanisms of cardiorespiratory arrests in epilepsy monitoring units (MORTEMUS): a retrospective study. *Lancet Neurol.*, **12**, 966–977.
27. McKinney, B.C., Chow, C.Y., Meisler, M.H. and Murphy, G.G. (2008) Exaggerated emotional behavior in mice heterozygous null for the sodium channel Scn8a (Nav1.6). *Genes Brain Behav.*, **7**, 629–638.
28. Liao, Y., Deprez, L., Maljevic, S., Pitsch, J., Claes, L., Hristova, D., Jordanova, A., Ala-Mello, S., Bellan-Koch, A., Blazevic, D. *et al.* (2010) Molecular correlates of age-dependent seizures in an inherited neonatal-infantile epilepsy. *Brain*, **133**, 1403–1414.
29. Osorio, N., Cathala, L., Meisler, M.H., Crest, M., Magistretti, J. and Delmas, P. (2010) Persistent Nav1.6 current at axon initial segments tunes spike timing of cerebellar granule cells. *J. Physiol.*, **588**, 651–670.
30. Kohrman, D.C., Harris, J.B. and Meisler, M.H. (1996) Mutation detection in the med and medJ alleles of the sodium channel Scn8a. Unusual splicing due to a minor class AT-AC intron. *J. Biol. Chem.*, **271**, 17576–17581.
31. Bender, A.C., Natola, H., Ndong, C., Holmes, G.L., Scott, R.C. and Lenck-Santini, P.P. (2013) Focal Scn1a knockdown induces cognitive impairment without seizures. *Neurobiol. Dis.*, **54**, 297–307.
32. Han, S., Tai, C., Westenbroek, R.E., Yu, F.H., Cheah, C.S., Potter, G.B., Rubenstein, J.L., Scheuer, T., de la Iglesia, H.O. and Catterall, W.A. (2012) Autistic-like behaviour in Scn1a+/− mice and rescue by enhanced GABA-mediated neurotransmission. *Nature*, **489**, 385–390.
33. Trudeau, M.M., Dalton, J.C., Day, J.W., Ranum, L.P. and Meisler, M.H. (2006) Heterozygosity for a protein truncation mutation of sodium channel SCN8A in a patient with cerebellar atrophy, ataxia, and mental retardation. *J. Med. Genet.*, **43**, 527–530.
34. Kearney, J.A., Buchner, D.A., De Haan, G., Adamska, M., Levin, S.I., Furay, A.R., Albin, R.L., Jones, J.M., Montal, M., Stevens, M.J. *et al.* (2002) Molecular and pathological effects of a modifier gene on deficiency of the sodium channel Scn8a (Na(v)1.6). *Hum. Mol. Genet.*, **11**, 2765–2775.
35. Sprunger, L.K., Escayg, A., Tallaksen-Greene, S., Albin, R.L. and Meisler, M.H. (1999) Dystonia associated with mutation of the neuronal sodium channel Scn8a and identification of the modifier locus Scnm1 on mouse chromosome 3. *Hum. Mol. Genet.*, **8**, 471–479.
36. Kohrman, D.C., Smith, M.R., Goldin, A.L., Harris, J. and Meisler, M.H. (1996) A missense mutation in the sodium channel Scn8a is responsible for cerebellar ataxia in the mouse mutant jolting. *J. Neurosci.*, **16**, 5993–5999.
37. Hawkins, N.A., Martin, M.S., Frankel, W.N., Kearney, J.A. and Escayg, A. (2011) Neuronal voltage-gated ion channels are genetic modifiers of generalized epilepsy with febrile seizures plus. *Neurobiol. Dis.*, **41**, 655–660.
38. Martin, M.S., Tang, B., Papale, L.A., Yu, F.H., Catterall, W.A. and Escayg, A. (2007) The voltage-gated sodium channel Scn8a is a genetic modifier of severe myoclonic epilepsy of infancy. *Hum. Mol. Genet.*, **16**, 2892–2899.
39. Sun, W., Wagnon, J.L., Mahaffey, C.L., Briese, M., Ule, J. and Frankel, W.N. (2013) Aberrant sodium channel activity in the complex seizure disorder of Celf4 mutant mice. *J. Physiol.*, **591**, 241–255.
40. Papale, L.A., Beyer, B., Jones, J.M., Sharkey, L.M., Tufik, S., Epstein, M., Letts, V.A., Meisler, M.H., Frankel, W.N. and Escayg, A. (2009) Heterozygous mutations of the voltage-gated sodium channel SCN8A are associated with spike-wave discharges and absence epilepsy in mice. *Hum. Mol. Genet.*, **18**, 1633–1641.
41. O'Brien, J.E., Sharkey, L.M., Vallianatos, C.N., Han, C., Blossom, J.C., Yu, T., Waxman, S.G., Dib-Hajj, S.D. and Meisler, M.H. (2012) Interaction of voltage-gated sodium channel Nav1.6 (SCN8A) with microtubule-associated protein Map1b. *J. Biol. Chem.*, **287**, 18459–18466.
42. Kehrl, J.M., Sahaya, K., Dalton, H.M., Charbeneau, R.A., Kohut, K.T., Gilbert, K., Pelz, M.C., Parent, J. and Neubig, R.R. (2014) Gain-of-function mutation in Gnao1: a murine model of epileptiform encephalopathy (EIEE17)? *Mamm. Genome*, **25**, 202–210.
43. Lee, C.H., Javed, D., Althaus, A.L., Parent, J.M. and Umemori, H. (2012) Neurogenesis is enhanced and mossy fiber sprouting arises in FGF7-deficient mice during development. *Mol. Cell. Neurosci.*, **51**, 61–67.
44. Nadler, J.J., Moy, S.S., Dold, G., Trang, D., Simmons, N., Perez, A., Young, N.B., Barbaro, R.P., Piven, J., Magnuson, T.R. *et al.* (2004) Automated apparatus for quantitation of social approach behaviors in mice. *Genes Brain Behav.*, **3**, 303–314.
45. de Kovel, C.G.F., Meisler, M., Brilstra, E.H., van Berkestijn, F.M., van t'Slot, R., van Lieshout, S., Nijman, I.J., O'Brien, J.E., Hammer, M.F., Estacion, M. *et al.* (2014) Characterization of a de novo SCN8A mutation in a patient with epileptic encephalopathy. *Epilepsy Res.*, doi:10.1016/j.eplepsyres.2014.08.020.
46. Larsen, J., Carvill, G.L., Gardella, E., Kluger, G., Schmiedel, G., Barisic, N., Depienne, C., Brilstra, E., Mang, Y., Nielsen, J.E.K. *et al.* (2014) The phenotypic spectrum of *SCN8A* encephalopathy. *Neurology*, in press.